Available online at www.sciencedirect.com

ScienceDirect

Acta Materialia 58 (2010) 6452–6463

Acta MATERIALIA

www.elsevier.com/locate/actamat

Texture development in near-α Ti friction stir welds

R.W. Fonda *, K.E. Knipling

Naval Research Laboratory, Code 6356, 4555 Overlook Avenue, SW, Washington, DC 20375, USA

Received 8 June 2010; received in revised form 6 August 2010; accepted 7 August 2010

Abstract

The microstructures and crystallographic textures produced during friction stir welding of the near-α Ti-5111 titanium alloy were characterized as a function of welding speed. The textures produced were compared with ideal hexagonal close packed (hcp) shear textures and with predicted textures of hcp Burgers variants of ideal body-centered cubic (bcc) shear textures, showing that the deposited welds are dominated by the hcp P_1 and bcc D_1 textures. The hcp P_1 shear texture was dominant at slow weld speeds, while the bcc D_1 shear texture was dominant at the fast weld speed. This variation appears to result from a poor transmission of the shear deformation from the rotating tool to the deposited weld that develops at faster welding speeds. These observations are compared to other studies of friction stir welds in hcp and bcc materials reported in the literature.
Published by Elsevier Ltd. on behalf of Acta Materialia Inc.

Keywords: Friction stir welding; Shear texture; Titanium alloys; Electron backscattering diffraction (EBSD)

1. Introduction

Friction stir welding (FSW) is a solid-state joining technique that was developed by the Welding Institute (TWI) in 1991 [1] and has rapidly developed into a commercially important joining process for aluminum alloys [2,3]. In FSW, a rotating tool is translated along a joint line to “stir” together the two sides of the joint. The rotating tool heats the surrounding material through frictional and adiabatic heating, softening it and enabling its transfer around the tool and into the tool's wake. Using an appropriate tool design and welding parameters, the deposited material consolidates into a defect-free weld behind the tool (see Fig. 1).

The rotating FSW tool introduces shear deformation into the surrounding material [4]. While there has been considerable work on the crystallographic textures that develop during shear deformation of face-centered cubic (fcc) materials [5–11], much less attention has been devoted to shear textures developed in body-centered cubic (bcc) materials. The four primary bcc shear textures, later designated D, E, F, and J (see Table 1), were initially reported by Backofen and Hundy [12] in torsion studies of Armco iron. Subsequent studies of this alloy only reported the presence of two [6] or three [8] of these textures, but a detailed analysis using crystal plasticity theory and experimental torsion tests of three iron alloys by Baczynski and Jonas [13] confirmed the four ideal orientations and described their locations along the torsion fibers. That study also determined that the $D_2(\bar{1}\,\bar{1}\,2)[1\,1\,1]$ shear texture component (in Baczynski and Jonas' notation) dominates at elevated temperatures.

More recently, Li et al. [14] observed these shear textures after simulated equal channel angular extrusion (ECAE) of a bcc material. They, however, revised the notation of the bcc ideal shear orientations in order to reinforce the similarities with the more established fcc shear textures. Their designations switched the D_1 and D_2 orientations and used E, $\bar{E}$, J, and $\bar{J}$ in place of Baczynski and Jonas' E_2, E_1, J_2, and J_1, respectively, emphasizing that the bcc shear planes and directions are related to the fcc shear planes and directions simply through an exchange of the *hkl* and *uvw* indices. Thus, the new bcc $D_1(\bar{1}\,\bar{1}\,2)[1\,1\,1]$ shear texture bears an obvious resemblance to the fcc $A_1^*(1\,1\,1)[\bar{1}\,\bar{1}\,2]$ orientation, the bcc $E(1\,1\,0)[1\,\bar{1}\,1]$ corresponds to the fcc

* Corresponding author. Tel./fax: +1 202 767 2622.
E-mail address: richard.fonda@nrl.navy.mil (R.W. Fonda).

1359-6454/$36.00 Published by Elsevier Ltd. on behalf of Acta Materialia Inc.
doi:10.1016/j.actamat.2010.08.007

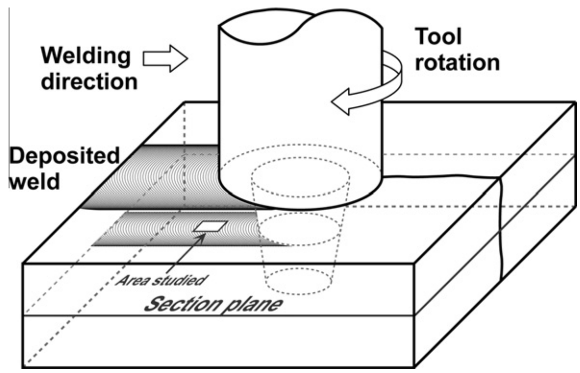

Fig. 1. Schematic of the friction stir welding process.

A($1\,\bar{1}\,1$)[$1\,1\,0$], and the bcc J($1\,1\,0$)[$1\,\bar{1}\,2$] corresponds to the fcc B($1\,\bar{1}\,2$)[$1\,1\,0$] orientation. Pole figures of these ideal bcc shear orientations are shown in Fig. 2. Li et al.'s [14] revised texture designations are used throughout this paper unless otherwise specified.

Only recently have there been any examinations of shear textures in hexagonal close packed (hcp) materials. The initial analysis of these textures was reported in 2007 by Beausir et al. [15], who used crystal plasticity theory to determine the ideal shear orientations and their persistence characteristics in hcp materials in simple shear, and compared those results to the experimental textures produced during torsion testing of a magnesium alloy. The possible hcp simple shear textures consist of five fibers, named B, P, Y, C_1, and C_2, and the end orientation of the P fiber, named P_1 (see Table 1). Beausir et al., however, demonstrated that the Y fiber is only convergent from $30° \leqslant \varphi_2 < 60°$ and that only one of the C fibers is convergent. Furthermore, they indicated that the large rotation vectors around the Y and C fibers would prevent any significant intensities from developing around those fibers. A similar analysis performed by Li [16] additionally predicted two possible twin-induced shear fibers, which were labeled h5 and h6, and determined the most stable orientations along

Table 1
Ideal crystallographic orientations of bcc [14] and hcp [15,16] simple shear deformation textures with Euler angles (Bunge's notation) from the $\varphi_2 = 0°$ and $\varphi_2 = 45°$ sections when applicable.

	Texture	Description	Euler angles (°)		
			φ_1	Φ	φ_2
bcc	D_1	$\{\bar{1}\,\bar{1}\,2\}\ \langle 1\,1\,1\rangle$	54.7/234.7	45	0
			144.7/324.7	90	45
bcc	D_2	$\{1\,1\,\bar{2}\}\ \langle 1\,1\,1\rangle$	125.3/305.3	45	0
			35.3/215.3	90	45
bcc	E	$\{1\,1\,0\}\ \langle 1\,\bar{1}\,1\rangle$	90	35.3	45
bcc	$\bar{E}$	$\{1\,1\,0\}\ \langle \bar{1}\,1\,\bar{1}\rangle$	270	35.3	45
bcc	F	$\{1\,1\,0\}\ \langle 0\,0\,1\rangle$	0/180	45	0
			90/270	90	45
bcc	J	$\{1\,1\,0\}\ \langle 1\,\bar{1}\,2\rangle$	90/210/330	54.7	45
bcc	$\bar{J}$	$\{1\,1\,0\}\ \langle \bar{1}\,1\,\bar{2}\rangle$	30/150/270	54.7	45
hcp	B-fiber	$\{0\,0\,0\,1\}\ \langle uvjw\rangle$	0	90	0–60
hcp	P-fiber	$\{hkil\}\ \langle 1\,1\,\bar{2}\,0\rangle$	0	0–90	0
hcp	P_1	$\{\bar{1}\,1\,0\,0\}\ \langle 1\,1\,\bar{2}\,0\rangle$	0	0	0
hcp	Y-fiber	c-axis tilted $\pm$ 30° towards SP	0	30	30–60
hcp	C_1-fiber	c-axis tilted $-30°$ towards SP from SD	60	90	0–60
hcp	C_2-fiber	c-axis tilted 30° towards SP from SD	120	90	0–60
hcp	h5-fiber {Li-2008-1031}	$\{hkil\}\ \langle 1\,1\,\bar{2}\,0\rangle$	85	90	0–60
hcp	H6-fiber {Li-2008-1031}	$\{\bar{1}\,1\,0\,0\}\ \langle 1\,1\,\bar{2}\,0\rangle$	140	90	0–60

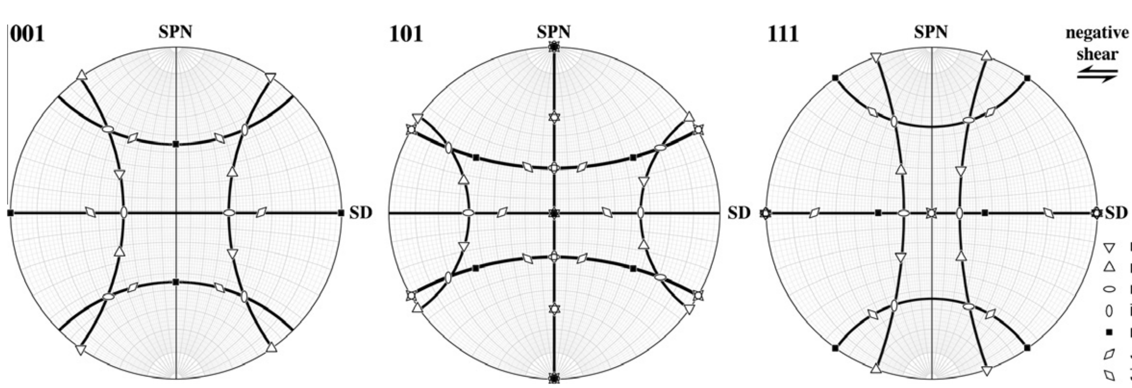

Fig. 2. Pole figures showing the important ideal orientations associated with simple shear deformation of bcc materials (after Baczynski and Jonas [13] and Li et al. [14]).